



## A Semi-Automatic Hybrid Approach for Defective Skulls Reconstruction

Antonio Marzola<sup>1</sup> , Lapo Governi<sup>2</sup> , Lorenzo Genitori<sup>3</sup> , Federico Mussa<sup>4</sup> , Yary Volpe<sup>5</sup> ,  
and Rocco Furferi<sup>6</sup> 

<sup>1</sup>University of Florence, [antonio.marzola@unifi.it](mailto:antonio.marzola@unifi.it)

<sup>2</sup>University of Florence, [lapo.governi@unifi.it](mailto:lapo.governi@unifi.it)

<sup>3</sup>Children's Hospital A. Meyer of Florence, [lorenzo.genitori@meyer.it](mailto:lorenzo.genitori@meyer.it)

<sup>4</sup>Children's Hospital A. Meyer of Florence, [federico.mussa@meyer.it](mailto:federico.mussa@meyer.it)

<sup>5</sup>University of Florence, [yary.volpe@unifi.it](mailto:yary.volpe@unifi.it)

<sup>6</sup>University of Florence, [rocco.furferi@unifi.it](mailto:rocco.furferi@unifi.it)

Corresponding author: Yary Volpe, [yary.volpe@unifi.it](mailto:yary.volpe@unifi.it)

**Abstract.** In cranioplasty surgery, achieving an effective aesthetic shape restoration of the cranial vault is the most important issue to ensure a proper outcome in terms of social and psychological benefits for the patient. To date, the most advanced approach uses CT/MRI data to reconstruct, in a pre-operative stage, the 3D anatomy of the defective skull in order to design a patient-specific prosthesis. In the last years, several techniques have been proposed to improve the applicability of such approach in the clinical practice, but the analysis of the related literature shows still open issues, due to the wide anatomical variability and complexity of the craniofacial anatomy that needs to be retrieved.

With the aim to overcome the State-of-the-Art drawbacks, a new semi-automatic *hybrid* procedure for repairing unilateral or quasi-unilateral (i.e. a single defect slightly passing the sagittal plane) cranial defects is presented. The novel approach is *hybrid* because a surface interpolation for filling the hole is used together with a template-based reconstruction guided by the healthy counterpart. The procedure, being landmark-independent and avoiding any patch adaptation, represents a valid alternative for the existing approaches also in terms of user's burden, requiring less time consuming and less cumbersome operations.

In addition, a new evaluating technique able to measure the symmetry of the reconstruction as well as the continuity between patch and healthy bone is proposed to test the procedure performance. Several test cases have been then addressed to prove the effectiveness and repeatability of the proposed procedure in reconstructing large-size defects of the skull.

**Keywords:** Reverse Engineering, CAD, Skull Reconstruction, Cranioplasty.

**DOI:** <https://doi.org/10.14733/cadaps.2020.190-204>

## 1 INTRODUCTION

As widely recognized, cranioplasty is a neurosurgical technique to repair cranial defects, usually holes, by insertion of a cranial implant. Cranial defects are typically due to trauma, congenital dysmorphisms, or complications of a previous surgery. A good restoration of the cranial integrity is fundamental for the functionality and protection of the brain as well as for aesthetics: an incorrect reconstruction of the cranial shape can lead to psychological and social consequences in the patients that cannot be underestimated, especially in pediatrics [12]. For this reason, the cranial implant must have both an aesthetically coherent shape with respect to the healthy bone and a precise fit with the outer surface of the skull. These aspects are crucial for a successful intervention.

In the last years, materials and techniques used in cranioplasty have been known an astonish evolution. In the last years, materials and techniques used in cranioplasty have been known an astonish evolution. Xenograft or autograft implants are being replaced by devices built pre-operatively on the patient-specific (virtual or physical) anatomical reproduction [1].

In fact, the application of Reverse Engineering and Additive Manufacturing techniques in the medical field allows to design and manufacture customized prosthetics and implants starting from Computed Tomography (CT) and Magnetic Resonance Imaging (MRI). This evolution has brought to less implant's intra-operative adaptation need, with many advantages regarding the reduction of surgical time and the improvement of the clinical outcomes [9],[11]. In this scenario, the proper reconstruction of the missing area in defective anatomies is proving to be one of the most challenging tasks, mainly due to the wide variability and high complexity of the human anatomy. Therefore, several approaches have been proposed with the aim of providing a virtual coherent anatomical reconstruction of the cranial vault to be used for the pre-operative design of the corrective plate [3]. All the proposed procedures can be categorized into four different strategies:

- *Mirroring-based techniques* are based on the reflection of the healthy half of the cranial vault onto the defective one. Despite this approach is the simplest and exploits the patient's own data as a template, it requires a high user interaction to achieve a good fitting between the healthy skull and the reconstructive patch. In fact, such methods rely on the computation of the symmetry plane, the isolation of the healthy region corresponding to the defect, and the adjustment of the reconstructed patch on the defective side of the skull. Furthermore, it makes possible of dealing only with unilateral defects.
- *Surface Interpolation-based techniques* pursue the approximation of the missing area by fitting a mathematical function that smoothly interpolates across the hole. In this way, the corrective surface is forced to pass through the defect's edge points and to maintain an adequate curvature continuity with the neighbor healthy region. On the other hand, the lack of information able to guide the surface interpolation in the missing region does not allow to achieve a proper reconstruction when wider holes need to be repaired. Commonly, the wider the hole the flatter will be the patch. Consequently, this technique is not suitable to fill large holes.
- *Deformed Template-based Techniques* adopt an a-priori generated 3D template of the healthy human skull properly warped on the defective skull to model the missing cranial area. This approach is suitable for any kind of defects, but it requires high user interaction for a proper registration between the template and the defective model, as well as it requires a high computational cost. In fact, the method requires a set of landmarks used to map the template to the patient skull.
- *Slice-based techniques* use 2D diagnostic CT/MRI images to fit a mathematical closed curve to the bone contour in a slice-by-slice approach. The curve provides the missing area approximation in continuity with the edge of the defect smoothly fitting the healthy bone. As in the Surface interpolation, the lack of information within the missing area could affect a correct reconstruction. Additionally, there is the need to stack the curves obtained slice by slice to achieve the restored skull.

A review of the above mentioned methods is provided in [3]; all the presented approaches share weaknesses and limits that mainly are represented either by a high user interaction request (*Mirroring-based techniques* and *Deformed Template-based Techniques*) or the lack of data within the hole that could compromise an aesthetically acceptable reconstruction (*Surface Interpolation-based Techniques* and *Slice-based Techniques*).

In order to overcome these drawbacks, a new *hybrid* procedure is here proposed (see Figure 1). The aim of the procedure is the semi-automatic restoration of the outer surface for a unilateral defective skull, which preserves the symmetry as much as possible when compared to the healthy half. The presented approach is *hybrid* since a surface interpolation for filling the hole is used together with a template-based reconstruction guided by the healthy counterpart. This way, the template-based methods' ability in reconstructing a coherent cranial shape is exploited in addition of the repeatability ensured by an automatic reconstruction to improve the quality and the accuracy of the reconstruction.

Differently from standard *Deformed Template-based Techniques*, the presented procedure is landmark-independent. The selection of landmarks, in fact, is not a trivial task and requires expert users to be accomplished. Moreover, in the proposed approach, the user interaction is limited to an adequate preparation of the starting model and to the selection of a single point on the edge of the hole that needs to be repaired. This results in a less cumbersome and time-consuming procedure when compared with both the existing *Mirroring-based* and *Deformed Template-based* approaches. Furthermore, the method overcomes the main limitations of *Surface Interpolation-based techniques* since it also allows the restoration of large defects.

The proposed procedure has been implemented in an original software coded in MATLAB® and several test cases, of both synthetic and real defective skulls, are addressed in order to verify its capability in restoring large defects (>100cm<sup>2</sup>). Additionally, a new metric to evaluate the quality of the reconstruction outcome is proposed.

In the following sections, a step-by-step description of the procedure is reported.

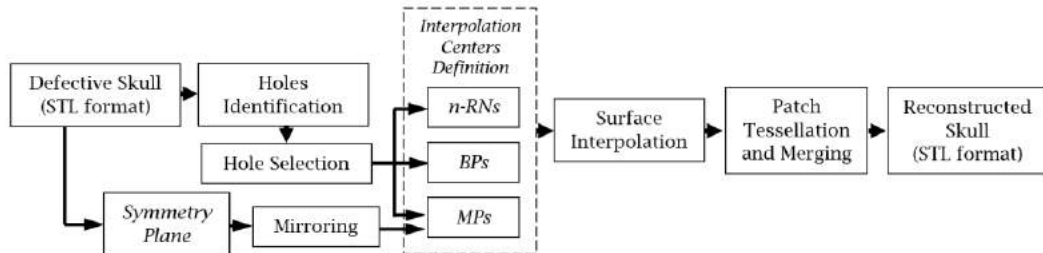


**Figure 1:** The proposed procedure.

## 2 METHODOLOGY

### 2.1 Starting Model in the STL Format

The developed procedure works on the surface mesh representing the defective skull in STL format obtained by a proper image segmentation from the patient's CT or MRI data. Dealing with hard tissues, the CT images are particularly suitable because bones appear with a well-identifiable greyscale intensity window. Therefore, a gray-value thresholding with an easily-recognizable lower and upper bound can be applied to filtering out the surrounding tissues from the region of interest. To date, much commercial software (e.g. Materialise Mimics or 3DSlicer) provide internal tools for such segmentation as well as for exporting the obtained 3D model in STL format.

Since the aim of the proposed algorithm is to restore the external shape of the cranial vault, the procedure requires only the external crust of the skull's mesh as input. For this reason, only the exterior poly-faces of the STL model are used as a starting mesh. Thanks to the regularity of

the cranial vault shape, the manual operations required to the exterior poly-faces selection is straightforward. This selection is automatically carried out by using a ray-tracing algorithm [13]. A proper number of rays outgoing in all direction starting from the centroid of the skull's model are imposed. The STL faces are set as fully transparent so that the surface mesh representing the external crust of the skull can be defined by the last triangle encountered by each ray. This way, the new mesh is no longer a 2-manifold watertight mesh (as resulting from the segmentation step) and each couple of vertices forming the defect boundary is connected by an edge not shared by two faces.

## 2.2 Identification of the Holes

Once the STL model of the external crust of the skull is available, the procedure firstly requires the identification of the boundary edge of the skull's defects. Two types of defects can be found, categorized as *simple* and *ring* holes [5]. A *simple hole* is characterized by only one boundary loop without any internal portions of bone (island), while a *ring hole* has internal islands and therefore at least two independent edges are present. Since during the segmentation a *ring hole* can be easily reduced into a *simple* one by removing the islands or making some bridges between the edges, the proposed approach deals only with *simple holes*.

For the edge identification, the properties of the STL are exploited, checking each edge of the mesh (i.e. each couple of connected points) and looking for the ones which are not shared by at least two triangles (Figure 2). Using such a procedure, the edges of all the holes on the skull are retrieved. Since the proposed procedure repairs only one defect at a time, in case more holes are detected the user is required to select one point on the edge of the hole to be filled (using a proper devised GUI). Starting from this selected point, the boundary loop of the defect under investigation is automatically defined.

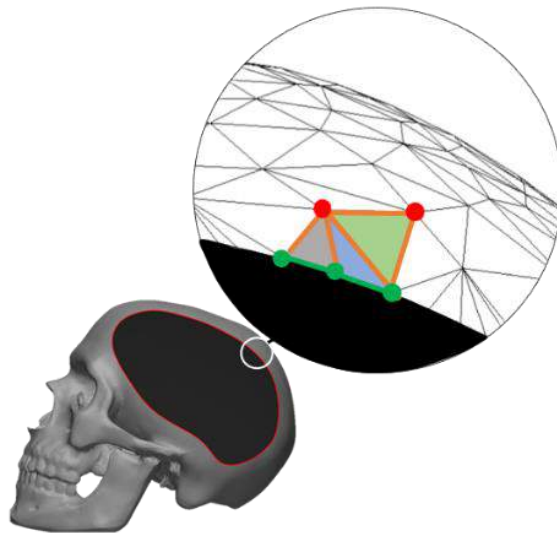


**Figure 2:** Automatic Edge Detection.

## 2.3 Symmetry Plane and Missing Points Definition

To achieve a reconstruction as symmetrical as possible, the healthy half is used as a template and mirrored around a properly defined plane, henceforward named *symmetry plane*, onto the defective one (Figure 3(a)). The definition of the *symmetry plane* is critical because it must ensure a precise superimposition between the template and the defective half. This allows to obtain an acceptable outcome both in terms of the continuity at the defect's boundary and of aesthetics. For

a reliable *symmetry plane* definition, in this application the method proposed by Di Angelo et al. in [6] is used, since it proved to be able to find a good approximation of skull's *symmetry plane* also in case of large defective area (i.e. in case of strong asymmetries). Furthermore, this method can be easily integrated into the proposed method, since it can work on the same STL on which the whole procedure works, without requiring further user's interaction.

Once the *symmetry plane* is defined and healthy part is mirrored onto the defective one (Figure 3(b)) the healthy half is used to obtain some meaningful points within the missing region (see Figure 4). As a consequence, this procedure strongly differs from traditional mirroring approaches since it does not encompass the use of the whole reconstructive patch. Such meaningful points, henceforward named *Missing Points (MPs)*, are used as nodes for the subsequent surface interpolation.

To this purpose, the first step is to extrapolate the MPs from the template; since the two halves are never perfectly superimposed, a simple Boolean subtract cannot be applied. Accordingly, the first step to extrapolate the *MPs* from the template consists of measuring the Euclidean Distance between each mirrored point and its nearest on the defective part. The nearest points are defined by means of k-Nearest Neighbors algorithm.

Only the mirrored points (*query points*) whose distances to the defective points (*reference points*) are greater than an imposed threshold  $r_a$  are kept, while the others are filtered out.  $r_a$  is an input of the procedure and represents the maximum distance to search the model's points as neighbors of the mirrored ones. Unfortunately, this step identifies the *MPs* of all the cranial holes. Therefore, only the *MPs* inside the selected boundary loop are considered.

Finally, points that are at a distance less than a certain value  $m$  from the edge itself are further filtered-out to detach *MPs* from the boundary.  $m$  represents the minimum distance (in mm) between the boundary and its nearest ring of the *MPs*, as showed in Figure 4. Too little value of  $m$  could affect the continuity between the skull and the reconstructive patch, while a too great value could be unable to lead to an acceptable outcome due to a lack of information within the hole.

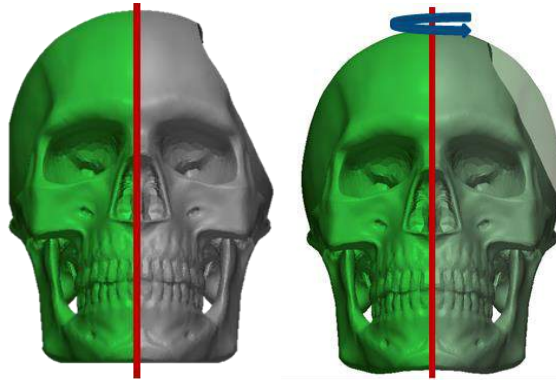


**Figure 3:** (a) *Symmetry plane* detection and (b) Mirroring of the healthy half onto the defective one.

#### 2.4 Definition of the Interpolation Centers

The actual definition of the restoration patch is obtained by means of a Surface Interpolation through a properly designed points-set. Considering the missing bone as a 3D surface described by a function  $f: \mathbf{R}^2 \rightarrow \mathbf{R}$  whose value  $f X_i$  is known only on a limited number of points  $\{X_i \in \mathbf{R}^2 : i=1,2,\dots,N\}$ , it can be approximated by a properly designed function  $s: \mathbf{R}^2 \rightarrow \mathbf{R}$  which satisfies at least the *interpolation condition*  $s X_i = f X_i$ .  $X_i$  are called *nodes of interpolation* or *interpolation*

centers, and represent the  $(x_i, y_i)$  coordinates of each vertex  $i$  in the STL model, while  $f X_i$  represent the correspondent  $z_i$  values.  $N$  is the total vertices number.

Several authors have proposed such approach for the cranial vault reconstruction using different interpolation strategies [3], but the surface  $s$  is usually defined with the  $X_i$  nodes represented only by the *Boundary Points (BPs)*, i.e. the vertices forming the edge of the defect that must be filled. This allows achieving the geometrical continuity between the skull and the reconstructed patch thanks to the *interpolation condition* but proves to be inadequate for the correction of large defects, since the information at the boundary is insufficient to guide a coherent reconstruction within the hole. As a result, the patch tends toward a too flat shape [5]. To overcome this limitation, the proposed approach uses not only the *BPs* but also the above-defined *MPs* as nodes of interpolation.

Furthermore, to ensure the continuity between the healthy bone and the corrective patch, an overlapping region between the reconstructed surface  $s$  and the healthy skull is created by adding the *n-Ring Neighbors (n-RNs)* of the boundary loop to the interpolation nodes i.e. the set of points within a given distance  $n$  lying in the outer side of the boundary (see Figure 4).  $n$  is a further input of the algorithm: the greater  $n$  the wider the overlapped region. However, the greater the set of points to be interpolated becomes, the greater is the computational time. Moreover, increasing  $n$  does not ensure a better reconstruction, since there is the possibility to exceed the cranial vault towards more complex areas (e.g. zygomatic or orbital region), thus increasing the complexity of the interpolation nodes.

Summing up, moving away from the SoA interpolation-based techniques that consider only the *BPs*, the proposed complete nodes-set  $X_i$  contains (Figure 4):

- *Boundary points (BPs)*: all the points  $(x_{BP}, y_{BP}, z_{BP})$  on the edge of the hole must be repaired.
- *Missing Points (MPs)*: all the points  $(x_{MP}, y_{MP}, z_{MP})$  of the healthy counterpart mirrored within the hole whose distance from the defect's edge is greater than  $m$ .
- *n-Ring Neighbors (n-RNs)*: the *n-Ring Neighbors* of the boundary loop, containing the points  $(x_{RN}, y_{RN}, z_{RN})$ .

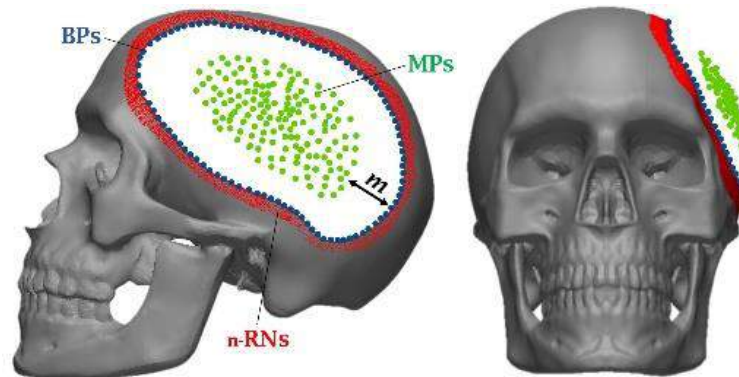


**Figure 4:** The Interpolation centers set: (a) lateral view, (b) frontal view.

## 2.5 Surface interpolation

Among the different surfaces  $s$  proposed in the related literature to solve the interpolation problem (e.g. Quartic Bézier Gregory Patch, Active Control, NURBS) [3], a Radial Basis Function (RBF) named Thin Plate Spline (TPS) have proved to be the most suitable for the proposed approach [4]. TPS is particularly adequate because ensures a  $C^1$  continuity, uses the *smoothest* interpolator of  $f$  and guarantee the lowest computational time. Furthermore, RBF impose few restrictions on the

nodes' geometry, being particularly suited to problems where the interpolation centers are represented by a set of scattered data with large data-free region. Using RBF, the interpolating function  $s \mathbf{X}$  is:

$$s \mathbf{X} = p \mathbf{X} + \sum_{i=1}^N \lambda_i \Phi \|\mathbf{X} - \mathbf{X}_i\| \quad (1)$$

As Equation (1) shows, RBF are described by the sum of  $N$  Radial Basis Functions  $\Phi$ , each associated with a different center  $\mathbf{X}_i$  and weighted by an appropriate coefficient  $\lambda_i$  plus a low-degree polynomial  $p$ .  $\|\cdot\|$  denotes the Euclidean norm. Regarding the Radial function  $\Phi$ , the specific Thin Plate Spline formulation is:

$$\Phi r = r^2 \log r \quad (2)$$

Using the TPS, the *interpolation condition* is avoided in favor of minimizing the energy functional  $E(s)$  (Equation (3)) over all interpolants  $\mathbf{X}_i$ .

$$E s = \int_{\mathbf{R}^2} \left[ \left( \frac{\partial^2 s}{\partial x^2} \right)^2 + \left( \frac{\partial^2 s}{\partial x \partial y} \right)^2 + \left( \frac{\partial^2 s}{\partial y^2} \right)^2 \right] dx dy \quad (3)$$

Avoiding a strict interpolation allows great advantages in terms of computational time, but an iterative refinement on the *Boundary Points* is required to ensure an adequate continuity between the bone and the patch. The iterations are stopped when the following condition is reached:

$$\left| f \mathbf{X}_{i,BP} - s \mathbf{X}_{i,BP} \right| < tol \quad (4)$$

Where  $f \mathbf{X}_{i,BP}$  is the  $f$  value known on each *BP* node,  $s \mathbf{X}_{i,BP}$  is the  $s$  value defined on each *BP* node and  $tol$  the maximum tolerance imposed for the whole set of *BPs*.

The tolerance is imposed only on the *BPs* since the *MPs* are only useful as a reference for the coherent shape restoration within the hole, while the *n-RNs* are used to ensure the right curvature at the boundary. That said, a direct comparison between the known  $f \mathbf{X}_i$  and the corresponding calculated  $s \mathbf{X}_i$  in all the test cases addressed (some of which are reported in the section 3) shows an approximation error ever less than  $10^{-1}$  mm with respect to the *MPs* and the *n-RN*, demonstrating a more than acceptable approximation even to the points not on the boundary.

## 2.6 Transformation of the Data

It has to be noticed that before the actual application of the surface interpolation, a proper alignment of the nodes  $\mathbf{X}_i$  to the global reference system, identified by the  $x$ ,  $y$  and  $z$  axes, is required. The aim is to obtain a new data-set where the interpolation points lie on a 2.5D surface. This ensures as far as possible a single-valued function  $s \mathbf{X}_i$  i.e. only a few points  $f \mathbf{X}_i$  share the same  $\mathbf{X}_i$  point.

Therefore, a rigid translation  $T_s$  is applied to the STL model until its centroid is on the center of the global reference system. Then, the best-fit plane  $\Pi_f$  through the points  $f \mathbf{X}_i$  is defined and the angle  $\theta$  between its normal  $\mathbf{n}_f$  and the direction  $z$  is measured. The angle  $\theta$  is used to apply a rigid rotation  $R_\theta$  to both the  $\mathbf{X}_i$  and the  $f \mathbf{X}_i$ . As a result, the normal vector of the  $\Pi_f$  is parallel to the  $z$  direction.

The actual application of the surface interpolation is then applied on the just-defined transformed nodes, named  $\mathbf{X}_i$ , with the corresponding transformed value  $f \mathbf{X}_i$ .

## 2.7 Patch Tessellation and Merging with the Defective Skull

Since the application of the TPS provides a mathematical surface exceeding the defect's boundary limits, the reconstructed patch is delimited using the boundary loop as defined in Section 2.2 (Figure 5).

Furthermore, being a mathematical surface, the delimited patch must be tessellated for the subsequent merging with the skull's STL model. The tessellation is carried out by a Crust-Based algorithm [2] defining a regular grid of nodes  $\{\chi_j \in \mathbf{R}^2 : j=1, 2, \dots, N\}$  in the  $xy$  plane. The resolution of the grid, from which directly depends the resolution of the reconstructive patch, is imposed similar to that of the original STL.

The tessellated patch is then rotated back to its original position, imposing a rotation guided by the  $\mathbf{R}_\theta^{-1}$  matrix. A complete re-mesh ensures the merging between the defective STL and the reconstructed patch. Finally, the inverse transformation  $T_s^{-1}$  is applied to the restored skull in order to return it to its initial position aligned with the original CT images.

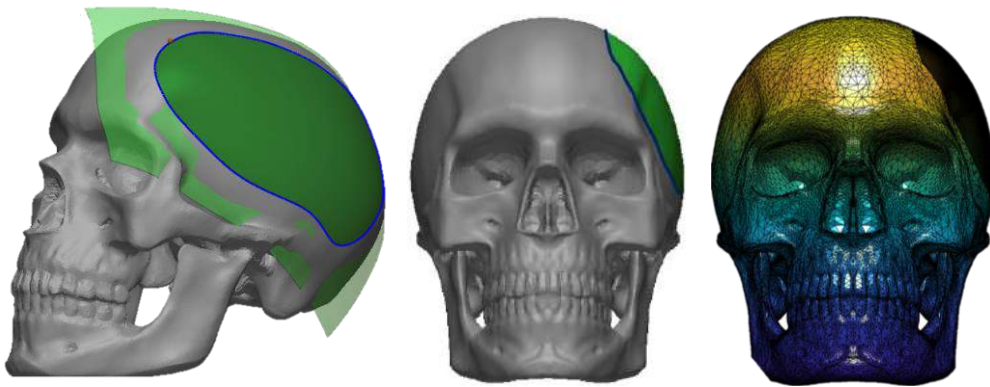


**Figure 5:** (a) Surface Interpolation. (b) surface delimitation using the boundary loop (in blue). (c) the final STL merged model.

## 3 RESULTS

In the related literature, the main criterion for evaluating a reconstructive patch is how closely it matches the original surface. For this purpose, usually the test cases addressed are represented by a complete skull with artificial holes [7] since the original surface of a real defective skull is rarely known. Notwithstanding, in the authors' view such comparison does not represent a good criterion for assessing the reconstruction outcome. At first analysis, it is not applicable in the normal clinical practice as the original surface is commonly unknown. More importantly, it does not consider the actual aesthetical outcome, which is the most relevant aspect in the cranial vault shape restoration [8], [10], [14].

Since a more symmetrical reconstruction is associated to a better outcome in terms of aesthetics, further investigations have been concerned with the implementation of quantitative evaluation criteria. Considering that the aim of the reconstruction must be the minimization of the cranial asymmetries as well as the surface continuity between the bone and the patch, regardless how close the restored skull is to the original surface, an alternative approach is here proposed. This approach is able to evaluate both the symmetry and the continuity of curvature of the restored cranial vault. In particular it allows both a quantitative evaluation of the skull asymmetry

by introducing a single index and a point-by-point map to evaluate the continuity of the entire cranial vault.

The asymmetry index is evaluated by means of the *Asymmetric Value (AV)* proposed in [6] and defined as:

$$AV = \text{median } \text{dist } p_j, TS PC_m \quad (5)$$

Where:

- $p_j$  is the  $j$ -th vertex belonging to the restored skull model. The Point-Cloud defined by the vertices of the restored skull model is named  $PC$ .
- $PC_m$  is the mirrored configuration of the  $PC$ .  $PC_m$  is found by reflecting  $PC$  upon the same *symmetry plane* used throughout the procedure (see Section 2.3).
- $TS(PC_m)$  is the tessellated surface obtained from the vertices  $PC_m$ .

As shown in Equation 5,  $AV$  represents the median of the distances between each point of the restored skull ( $p_j$ ) with respect to its closer tessellated surface triangle ( $TS(PC_m)$ ) of the mirrored configuration ( $PC_m$ ) of the restored skull itself. The  $AV$  is calculated as the median instead of the mean in order to reduce the weight of the natural little asymmetrical skull's regions in the calculation. The distance point-triangle permits to avoid the asymmetries due to the surface model sampling.

As mentioned above,  $AV$  provides a quantitative evaluation of the overall skull asymmetry: small value of the  $AV$  index means a symmetrical reconstruction and, consequently, an acceptable outcome.

In addition, the reconstruction consistency is checked also by looking for any discontinuities at the boundary between the bone and the reconstructed patch by means of the point-value of the  $AV$ , named  $AV_{point}$  and defined as [6]:

$$AV_{point} = \text{dist } p_j, TS PC_{m,i} \quad (6)$$

When applied throughout the cranial vault,  $AV_{point}$  provides the color map of the local asymmetries between the  $PC$  and the  $PC_m$ , suitable to highlight possible macroscopic discontinuities at the connection region between the bone and the patch.

It is worth to note that the proposed evaluation can be applied also to assess the reconstruction when the original healthy shape is completely unknown, that is as far commonly.

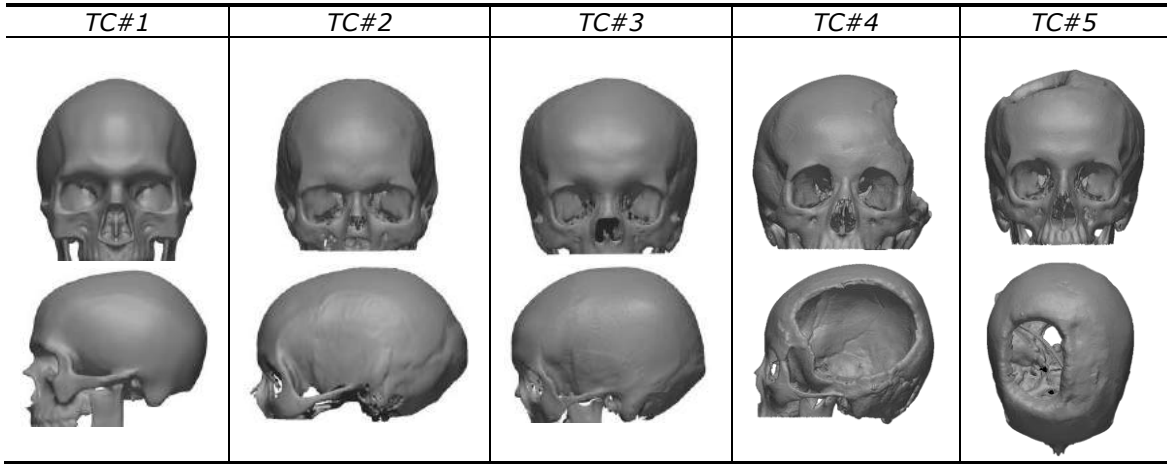
The new metrics ( $AV$  and  $AV_{point}$ ) have been applied to evaluate the accuracy of the proposed approach in the cranial shape restoration on several test cases. The CT images are provided by the Children's Hospital A. Meyer of Florence and include the neurocrania from Caucasians male and female aged between 11 and 33 years, both healthy and defective. For each test case, the skull bone has been segmented and exported in STL binary format by a skilled user by means of Materialise® Mimics' tools. The external crust of each STL is then isolated using Geomagic® Design X software. The obtained STL is used as an input for the described procedure, coded in MATLAB®.

In the following, the results of eight test cases are reported. As shown in Table 1, the reported test cases include:

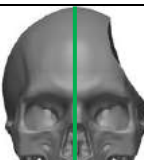
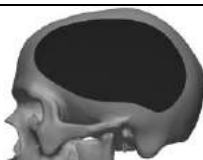
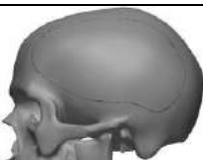
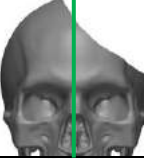
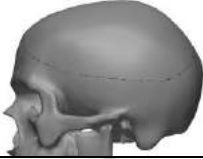
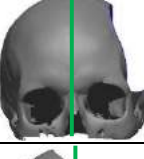
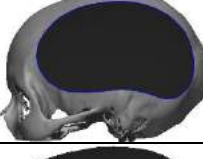
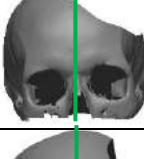
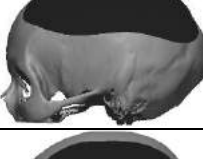
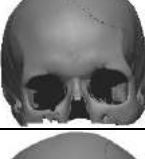
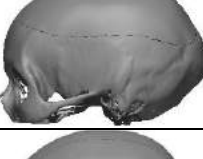
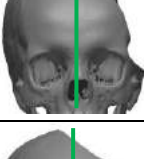
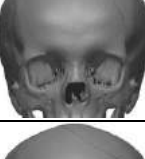
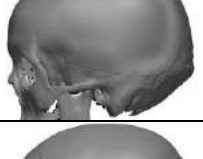
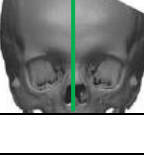
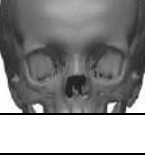
- TC#1 is a complete and perfectly symmetric synthetic skull.
- TC#2 and TC#3 are two real not defected skulls.
- TC#4 and TC#5 are real defective skulls: TC#4 is a purely unilateral large defect, while in TC#5 the defect slightly crosses the *symmetry plane* (see Table 2).

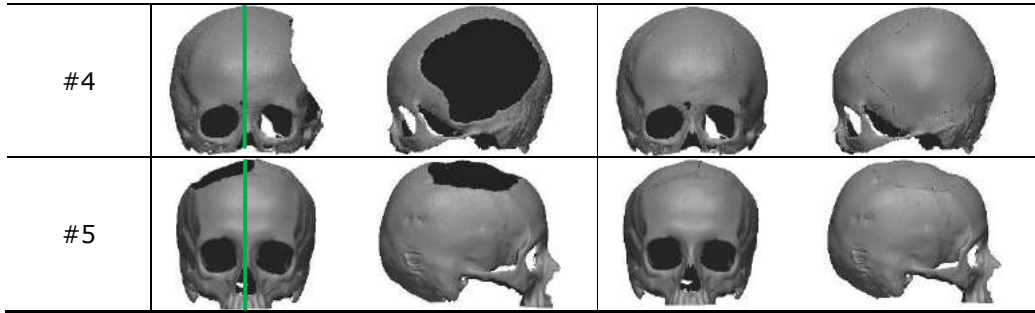
For each of the complete skulls (TC#1, TC#2 and TC#3), two different kinds of artificial defects are modeled: the first, named  $A$ , is purely unilateral, while the second, named  $B$ , slightly crosses the *symmetry plane* (see Table 2). In all cases, the defective area is greater than 100 cm<sup>2</sup>. Being actually defected skulls, cases TC#4 and TC#5 are not further modified.

Regarding the procedure's inputs, after a tuning of threshold parameters experimentally assessed,  $r_a$  is imposed equal to 10mm,  $m$  equal to 18mm and  $n$  equal to 50. Finally,  $tol$  is imposed equal to 10<sup>-2</sup>, that represents a good compromise between accuracy, if compared with the CT maximum resolution (around 0.5 mm), and calculation time.



**Table 1:** Starting model for the assessed test cases.

Test Case	Defective Frontal view	Defective Lateral view	Restored Frontal view	Restored Lateral view
#1_A				
#1_B				
#2_A				
#2_B				
#3_A				
#3_B				



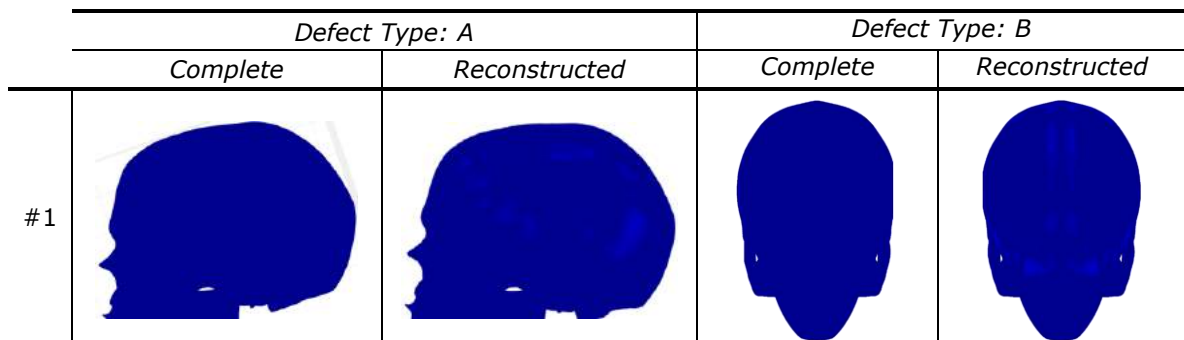
**Table 2:** Algorithm outcomes.

Table 2 reports the outcomes of the presented algorithm applied to the considered test cases. Evaluating the AV, Table 3 shows that the proposed procedure provided reconstructed models with an AV even lower than the original ones, where the comparison is possible. Where the original shape was unknown (TC#4 and TC#5), the low value of AV still allows to demonstrate the symmetry of the reconstruction and, consequently, allows a quantitative evaluation of the reconstruction acceptability.

The  $AV_{point}$  maps are reported in Table 4 and confirm the effectiveness of the reconstruction in terms of symmetry of the outcome as demonstrated by the larger dark blue areas in the reconstructed skulls compared to the originals. In addition, Table 4 shows the lack of any kind of discontinuities or asymmetries at the interface between healthy skull and reconstructive patch as evidenced by the absence of sudden color variations on the cranial surface.

Test Cases	Undefective	Def A	Def B
#1	0.000 mm	0.000 mm	0.000 mm
#2	0.898 mm	0.328 mm	0.169 mm
#3	0.945 mm	0.614 mm	0.360 mm
#4	N.A.	0.574 mm	N.A.
#5	N.A.	N.A.	0.691 mm

**Table 3:** AV values for all the test cases presented.



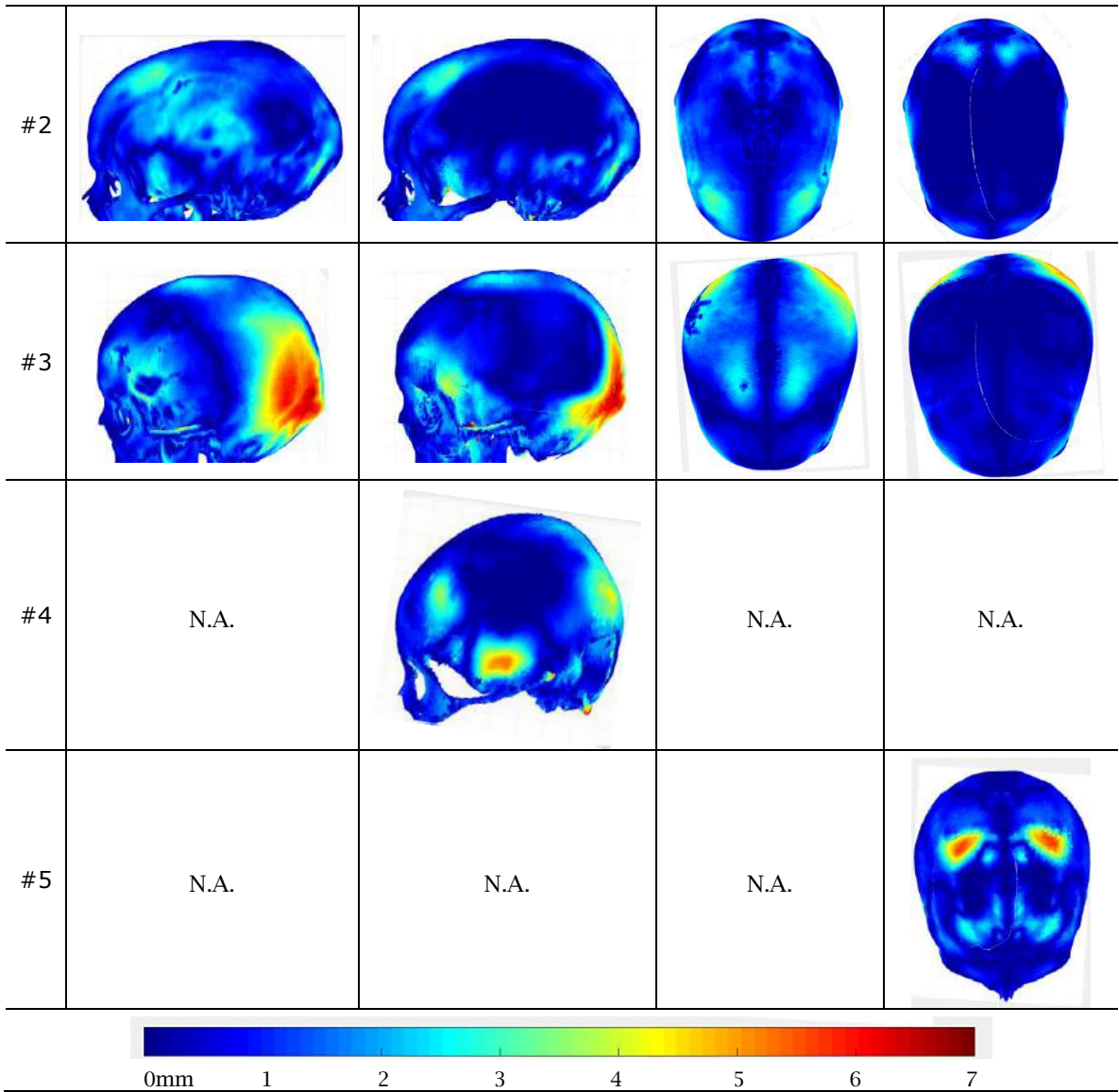


**Table 4:**  $AV_{point}$  map for all the test cases presented.

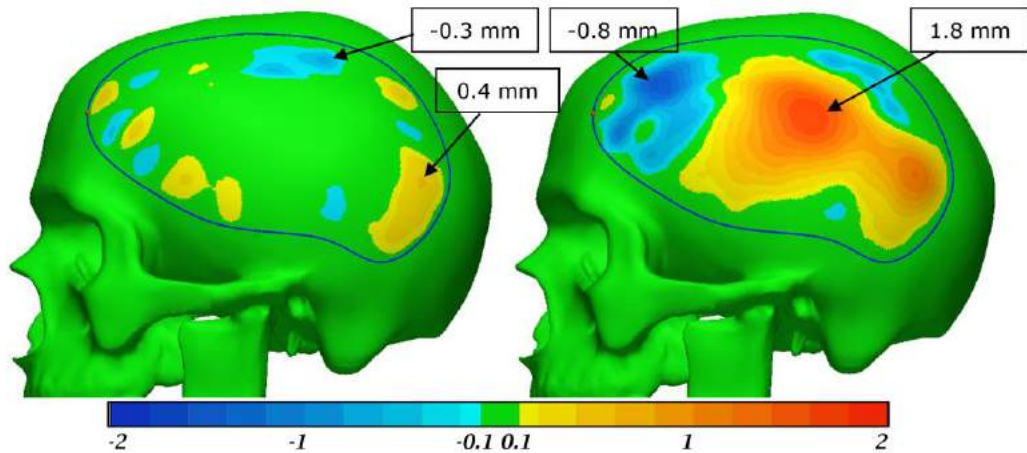
In order to perform a further assessment of the proposed procedure, a direct comparison between the reconstructed cranial vault and a properly designed reference skull has been also performed. To obtain reliable results, such reference shape must be able to minimize all the possible variables that could affect the final assessment, such as the natural asymmetry of a real cranial vault shape. For this aim, TC#1 has been chosen as reference skull: thanks to its perfect symmetry, this model allows to avoid all the external factors that could affect the reconstruction, limiting the evaluation only to the specific behavior of the procedure developed. Consequently, specifically for TC#1 the closer the reconstructed surface gets to the original shape, the better the reconstruction will be.

Figure 6 and Figure 7 show such a comparison in terms of mesh deviation between the starting model and the reconstructed one for, respectively, cases #1\_A and #1\_B. The reconstruction has been carried out both using the presented procedure (Figure 6(a) and Figure 7(a)) and the hole-

filling tool provided by Geomagic® Design X (Figure 6(b) and Figure 7(b)). The procedure's inputs value (i.e.  $r_a$ ,  $m$ ,  $n$  and  $tol$ ) are defined as above. As expected, the reconstruction achieved by adding the *MPs* yields a shape very close to the original model, providing a better outcome than the one yields by Design X and guided only by the *BPs*.

As shown in Figure 6(a) and 7(a) the deviation in the middle of the hole, where the reconstruction is driven by the *MPs*, is about 0 mm, while the reconstructed surface deviates slightly from the reference in the area close to the edge. In this area, the *MPs* are not considered to ensure a better continuity at the defect's edge when the perfect symmetry of the cranial vault is not verified, that means in all the real cases.

In conclusion, all the evaluations proved the procedure ability to provide an aesthetically coherent outcome ensuring both mathematical continuity at the boundary of the defect and a symmetric reconstruction with respect to the healthy counterpart.



**Figure 6:** TC#1\_A – The comparison between the complete symmetric synthetic skull and the reconstructed carried out by (a) the proposed method and (b) the hole-filling tool provided by using Geomagic® Design X.

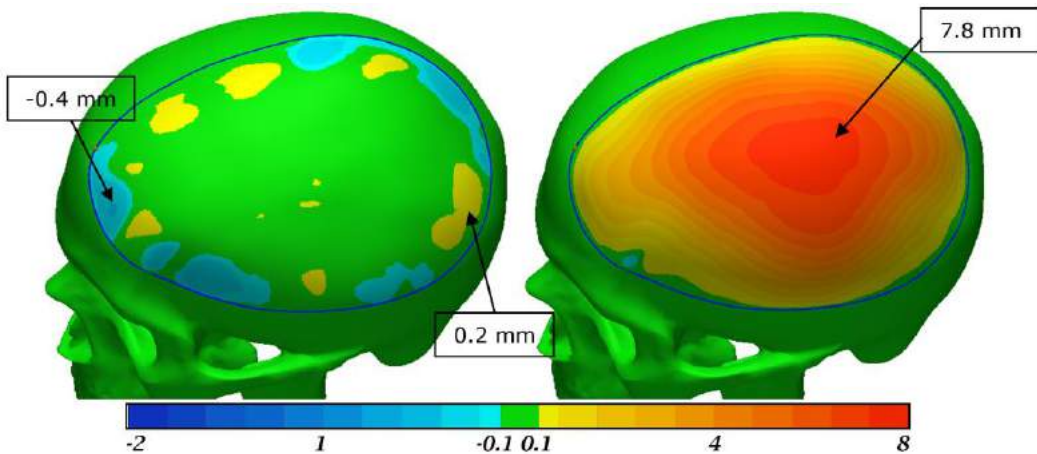


**Figure 7:** TC#1\_B – The comparison between the complete symmetric synthetic skull and the reconstructed carried out by (a) the proposed method and (b) the hole-filling tool provided by using Geomagic® Design X.

#### 4 DISCUSSION AND CONCLUSIONS

To date, one of the toughest tasks in the cranioplasty surgery is the pre-operative virtual design of a corrective plate. To ensure an acceptable aesthetical and functional outcome, such a design must be based on a proper anatomical reconstruction usually done in virtual environments by skilled operators.

Several techniques have been developed for the cranial vault reconstruction, but all of them shared some drawbacks (e.g. too complex or time-consuming operations or incorrect resulting geometries) that limit their applicability. The difficulty is mainly due to the lack of information in the missing area and the complexity of the shape that must be restored. In order to overcome these drawbacks, a novel hole-filling procedure for the restoration of unilateral defective skulls was presented. The procedure is suited for unilateral or quasi-unilateral (i.e. a single defect slightly passing the sagittal plane) large defects.

The innovative idea was to use the mirrored healthy counterpart as a template to obtain some meaningful points in the missing region to guide the subsequent reconstruction carried out by a Surface Interpolation-based technique. The procedure works automatically starting from the external poly-faces of the defective skull, leaving to the user only the selection of the hole to be repaired by clicking one point on its edge. Being landmark-independent and avoiding any patch adaptation, the developed procedure represents a valid alternative for the existing approaches in terms of user's burden, requiring less time consuming and less cumbersome operations.

The test cases addressed show that the novel procedure leads to a very symmetric reconstruction with regards to the healthy counterpart, ensuring a consistent aesthetic outcome.

As regards the computational time starting from the properly modified STL, it is closely related to the resolution of the surface model (number of vertices forming the STL file). For the addressed test cases, the computational time was between 10 and 25 minutes for point sets from 80,000 to 120,000. The slower step is the symmetry plane definition, which requires at least 80% of the total computational burden. In order to improve the applicability of the procedure by making it fully automatic, future efforts must concern the automatization of the external poly-faces selection.

Future work should also concern the extension of the procedure applicability to all kinds of defects, including the bilateral ones. With this aim, further studies could assess a mean shape undefective skull instead of the healthy counterpart as a template, similarly to the Deformed Template-based techniques. As with the Mirroring-Based technique, basing the reconstruction upon the *MPs* and the subsequent surface interpolation instead of using the whole template could overcome some limitation of the Deformed Template techniques, ensuring the skull surface continuity without time-consuming user's operations.

Antonio Marzola, <http://orcid.org/0000-0002-7842-4562>

Lapo Governi, <http://orcid.org/0000-0002-7417-3487>

Lorenzo Genitori, <http://orcid.org/0000-0002-4359-0798>

Federico Mussa, <http://orcid.org/0000-0003-3156-2543>

Yary Volpe, <http://orcid.org/0000-0002-5668-1912>

Rocco Furferi, <http://orcid.org/0000-0001-6771-5981>

#### REFERENCES

- [1] Aydin, S.; Kucukyuruk, B.; Abuzayed, B.; Aydin, S.; Sanus, G. Z.: Cranioplasty: Review of materials and techniques, *Journal of Neurosciences in Rural Practice*, 2(2), 2011, 162-167. <https://doi.org/10.4103/0976-3147.83584>
- [2] Amenta, N.; Bern, M.; Kamvyselis, M.: A new voronoi-based surface reconstruction algorithm, *Proceedings of the 25th Annual Conference on Computer Graphics and Interactive Techniques, SIGGRAPH*, 1998, 415-422. <https://doi.org/10.1145/280814.280947>

- [3] Buonamici, F.; Furferi, R.; Genitori, L.; Governi, L.; Marzola, A.; Mussa, F.; Volpe, Y.: Reverse engineering techniques for virtual reconstruction of defective skulls: An overview of existing approaches, *Computer-Aided Design and Applications*, 16(1), 2018, 103-112. <https://doi.org/10.14733/cadaps.2019.103-112>
- [4] Carr, J. C.; Fright, R.; Beatson, R. K.: Surface interpolation with Radial Basis Function for medical imaging, *IEEE Transaction on Medical Imaging*, 16(1), 1997, 96-107. <https://doi.org/10.1109/42.552059>
- [5] Chong, C. S.; Lee, H. P.; Kumar, S.: Automatic hole repairing for cranioplasty using Bézier surface approximation, *Journal of Craniofacial Surgery*, 17(2), 2006, 344-352. <https://doi.org/10.1097/100001665-200603000-00024>
- [6] Di Angelo, L.; Di Stefano, P.; Governi, L.; Marzola, A.; Volpe, Y.: A robust and automatic method for the best Symmetry Plane detection of the craniofacial skeletons, *Symmetry*, 11(2), 2019, 245. <https://doi.org/10.3390/sym11020245>
- [7] Fuessinger, M. A.; Schwarz, S.; Cornelius, C.-P.; Metzger, M. C.; Ellis, E.; Probst, F.; Semper-Hogg, W.; Gass, M.; Schlager, S.: Planning of skull reconstruction based on a statistical shape model combined with geometric morphometrics, *International Journal of Computer Assisted Radiology and Surgery*, 13(4), 2018, 519-529. <https://doi.org/10.1007/s11548-017-1674-6>
- [8] Gangestad, S. W.; Thornhill, R.; Yeo, R. A.: Facial attractiveness, developmental stability, and fluctuating asymmetry. *Ethology and Sociobiology*, 15(2), 1994, 73-85. [https://doi.org/10.1016/0162-3095\(94\)90018-3](https://doi.org/10.1016/0162-3095(94)90018-3)
- [9] Girod, S.; Teschner, M.; Schrell, U.; Kevekordes, B.; Girod, B.: Computer-aided 3D simulation and prediction of craniofacial surgery: a new approach, *Journal of Cranio-Facial Surgery*, 29(3), 2001, 156-158. <https://doi.org/10.1054/jcms.2000.0203>
- [10] Grammar, K.; Thornhill, R. Human facial attractiveness and sexual selection: The role of averageness and symmetry. *Journal of Comparative Psychology*, 108(3), 1994, 233-242. <http://dx.doi.org/10.1037/0735-7036.108.3.233>
- [11] Maravelakis, E.; David, K.; Antoniadis, A.; Manios, A.; Bilalis, N.; Papaharilaou, Y.: Reverse engineering techniques for cranioplasty: A case study, *Journal of Medical Engineering and Technology*, 32(2), 2008, 115-121. <https://doi.org/10.1080/03091900600700749>
- [12] Meyer-Marcotty, P.; Alpers, G.W.; Gerdes, A. B. M.; Stellzig-Eisenhauer, A.: Impact of facial asymmetry in visual perception: A 3-dimensional data analysis, *American Journal of Orthodontics and Dentofacial Orthopedics*, 137, 2010, 168.e1-168.e8. <https://doi.org/10.1016/j.ajodo.2008.11.023>
- [13] Möller, T.; Trumbore, B.: Fast, minimum storage ray-triangle intersection, *Journal of Graphics Tools*, 2(1), 1997, 21-28. <https://doi.org/10.1080/10867651.1997.10487468>
- [14] Penton-Voak, I.S.; Jones, B.C.; Little, A.C.; Baker, S.; Tiddeman, B.; Burt, D.M.; Perrett, D.I.: Symmetry, sexual dimorphism in facial proportions and male facial attractiveness, *Proceedings of the Royal Society Biological Sciences*, 268 (1476), 2001, 1617-1623. <https://doi.org/10.1098/rspb.2001.1703>